Quim. Nova, Vol. 47, No. 9, e-20240052, 1-8, 2024 http://dx.doi.org/10.21577/0100-4042.20240052

Article

EFFICIENT AND REUSABLE MATERIALS WITH PYROCHLORE STRUCTURE FOR REMOVING RED DYE FROM AQUEOUS MEDIA

Valber E. S. Firmino[a], Júlia B. R. Fernandes[a], Marcelo J. B. Souza[b] and Anne M. Garrido Pedrosa[a,*]

[a]Programa de Pós-Graduação em Química, Universidade Federal de Sergipe, 49107-230 São Cristóvão – SE, Brasil

[b]Departamento de Engenharia Química, Universidade Federal de Sergipe, 49107-230 São Cristóvão – SE, Brasil

Received: 04/01/2024; accepted: 06/13/2024; published online: 07/24/2024

Mixed oxides of pyrochlore structure of the type $La_2Zr_2O_7$ and $La_2M_{0.3}Zr_{1.7}O_7$ (M = Fe or Ni) were synthesized through the modified proteic method and calcined at 900 °C for 2 h, this is a synthesis route not yet explored for materials with this structure and were characterized by X-ray diffraction, scanning electron microscopy images, point of zero charge (PZC) and specific surface area. Its abilities to remove pollutants from aqueous media by adsorption process were investigated using a model compound. Data analysis revealed that the synthesized materials correspond to the pyrochlore phase ($La_2Zr_2O_7$). They present particulate morphology with grains of different sizes and pores in their structure. The results of the adsorption studies show that the materials are efficient adsorbents for the removal of model compound in aqueous media, with efficiency above 90%. The adsorption kinetics of the compound in the adsorbents was studied. The materials were applied in reuse studies five times and maintained high efficiencies, highlighting the better performance presented by the material without doping. The obtained adsorbents were also submitted to removal of contaminants of industrial effluent tests and compared with the silica gel and activated carbon materials and also proved to be promising materials.

Keywords: modified proteic method; pyrochlore structure; contaminants; materials reuse.

INTRODUCTION

The use of mixed oxides with perovskite or spinel structures in various processes has increased in recent years, such as in catalysis[1-3] and, more recently, in the removal of contaminants from effluents by adsorption.[4-7] One of the contributors to the contamination of wastewater are compounds used in the dyeing processes of fabrics, which can be generating significative amounts of these unfixed compounds, and when they are improperly discarded contribute to the negative environmental impact of water.[8-10]

Several materials are used as adsorbents in wastewater pollutants removal processes, especially those that stand out for their good efficiency at low cost.[4,11-13] More recently, mixed oxides with a perovskite structure (with the general formula ABO_3) have been shown to be efficient adsorbents in the removal of compounds used in some industrial processes, such as Congo Red, turquoise blue, methylene blue, bezaktiv red and blue.[4-6,11-13]

Mixed oxides of the $A_2B_2O_7$ type pyrochlore structure are widely used in catalytic processes but reports of these oxides involved in adsorption processes of textile dyes were not currently found in the main search databases. In positions A and B of the pyrochlore structure, trivalent and tetravalent cations are usually found, or else A is divalent while B is pentavalent.[14-16] The formation of the pyrochlore structure can be affected by combinations of cations that occupy the A and B positions, presence of dopants, synthesis methods, among other factors.[15,16] The studies of obtain of materials with different combinations of cations in the pyrochlore structure, and optimized synthesis methods represent a scientific opportunity for the development and improvement of new nanomaterials with potential applications in adsorption processes, mainly with the possibility that they present advantages over the use of other conventional materials, obtaining greater efficiency in the adsorption process and possibility of reuse.

Among the various methods for synthesizing mixed oxides, the modified proteic method has gained relative prominence in recent years.[4-6,11-13,17,18] Considerably simple to perform compared to other methods for obtaining mixed oxides such as Pechini method, chelating precursors, mechanosynthesis or co-precipitation method, the modified proteic method ends up becoming viable due to its lower cost, lower processing temperatures, reduced steps, in addition to obtaining well-crystallized materials.[4,11,17,18]

In the case of the modified proteic method, the formation of the oxide typically occurs after the calcination of a complex precursor, obtained from a complexation of the chelating agent with the cations present in the solution. The chelating agent used with a high protein value is collagen, which is a relatively low-cost material and has been shown to be very effective in the formation of mixed oxides. The direct use of protein reduces reaction steps and favors the occurrence of inorganic polymer formation reactions.[4,5,17,18]

Recent studies[4,5,18] involving synthetic nanomaterials obtained by the modified protein used as adsorbent materials have highlighted their properties such as surface area, presence of active sites that favor interaction with the dye, stability and possibility of reuse with high efficiency.

The literature reports that the $La_2Zr_2O_7$ material has been previously prepared by the sol-gel and Pechini methods, but there are no reports of preparation by the modified proteic method. Rao *et al.*[19] investigated the obtaining of pyrochlore oxides of the $La_2Zr_2O_7$ type by the sol-gel method as a function of temperature and concluded that nanometric and bulky particles were obtained with temperatures above 800 °C. Haynes *et al.*[20] studied the catalytic properties of materials with a pyrochlore structure of the pure $La_2Zr_2O_7$ type and with Sr and Rh doping obtained by the Pechini method for the partial oxidation reaction of *n*-tetradecane aiming at the production of synthesis gas, however, they were only successful in the formation of the pyrochlore phase for the strontium-doped material.

Therefore, this work presents the synthesis of mixed oxides with pyrochlore structure, based on lanthanum and zirconium,

*e-mail: annemgp@gmail.com

Associate Editor handled this article: Cassiana C. Montagner

with iron or nickel doping through the modified proteic method, with promising results in obtaining the desired phase and at lower synthesis temperatures. In addition, an evaluation of the materials obtained for removing pollutants from aqueous media by adsorption process was also carried out, choosing the Congo Red[7,21] compound as representative (chemical formula $C_{32}H_{22}N_6Na_2O_6S_2$, Riedel-de Haen, São Paulo, Brazil) and evaluating the efficiency of the adsorbents prepared in reuse cycles. The study also evaluated the behavior of the developed adsorbents when subjected to industrial effluent containing a textile compound and also compared to other known adsorbents.

EXPERIMENTAL

Synthesis of the $La_2Zr_2O_7$ and $La_2M_{0.3}Zr_{1.7}O_7$ (M = Fe or Ni)

The materials $La_2Zr_2O_7$ and $La_2M_{0.3}Zr_{1.7}O_7$ (M = Fe or Ni) were synthesized through the proteic method modified by a methodology adapted from the literature[4,5,18] with some modifications.

The stoichiometric calculations for the synthesis of the materials were made with the objective of obtaining 2.0 g each after the calcination procedure. For the standard material $La_2Zr_2O_7$, the stoichiometric mass of hydrated zirconium nitrate (m = 1.796 g) ($ZrO(NO_3)2H_2O$, 99%, Scientific ACS, São Paulo, Brazil) was initially dissolved in 150 mL of distilled water under magnetic stirring at 30 °C for 30 min. Then, the stoichiometric mass of lanthanum nitrate hexahydrate (m = 3.058 g) ($La(NO_3)_2.6H_2O$, 99%, Dinâmica, São Paulo, Brazil) was added, keeping the system under the same temperature for another 30 min. After this period, the system was subjected to a temperature increase until it stabilized at 70 °C when the collagen (Stem pharmaceutical, Porto Alegre, Brazil) mass was added in a 1:1 ratio with the mass of the nitrates used. The system remained under magnetic stirring for 1 h and 30 min. After this period, the system was subjected to a heat treatment step for 2 h in a muffle furnace at 350 °C. The material obtained was macerated using a mortar and pestle forming the precursor powder. Part of this powder was calcined in a muffle furnace for 2 h at 900 °C and the other part was stored for later analysis.

To obtain materials with nominal composition $La_2M_{0.3}Zr_{1.7}O_7$ (M = Fe or Ni), the experimental procedure was similar to that described above, however, adding the stoichiometric mass of nickel(II) nitrate hexahydrate (m = 0.313 g) ($Ni(NO_3)_2.6H_2O$, 97%, Neon, São Paulo, Brazil) to obtain $La_2Ni_{0.3}Zr_{1.7}O_7$ and the stoichiometric mass of iron(III) nitrate nonahydrate (m = 0.440 g) ($Fe(NO_3)_3.9H_2O$, 98%, Synth, São Paulo, Brazil) to obtain $La_2Fe_{0.3}Zr_{1.7}O_7$ after addition of zirconium nitrate, with a small variation in the stoichiometric masses of the lanthanum and zirconium salts. Both materials were subjected to the same heat treatment and calcination procedures as the standard material. The precursor powders were named LZO350, LFZO350 and LNZO350 and the powders calcined at 900 °C of LZO900, LFZO900 and LNZO900.

Characterization of the synthesized compounds

X-ray diffraction analysis was performed using a Rigaku (Tokyo, Japan) DMAX100 diffractometer with CuKα radiation (λ = 1.5418 Å), 2θ in the range of 5 to 65°, 0.02 step and 1° min^{-1} sweep. The obtained diffraction patterns were compared with the ICSD (Inorganic Crystal Structure Database) patterns. scanning electron microscopy (SEM) images were obtained using a Hitachi High Technologies (Tokyo, Japan) equipment, model TM-3000 with magnifications in the range of 500 to 2000 times. The point of zero charge (PZC) was carried out using the balance method in a batch system. To determine the specific surface area by the Brunauer-Emmett-Teller (BET) method, the samples were subjected to degassing at 300 °C for 1 h and then an adsorption isotherm was obtained in Quantachrome equipment (Florida, USA), model NOVA 1200e. The Fourier transform infrared (FTIR) analyses were carried out in a Shimadzu (Tokyo, Japan) equipment, model IR-Prestige, in the wavenumber range between 4000 and 400 cm^{-1}, using the KBr based preparation method.

Contaminant removal tests

Before carrying out the adsorption tests, the analytical curve of the Congo Red (CR) solution in aqueous solution was constructed to obtain the absorbance of the solution as a function of its concentration, and a photodegradation study was carried out to evaluate the stability of the compound in the experimental conditions used. Both studies were performed in the absence of adsorbent material. In the scan applied in the range of 400 to 700 nm using a UV-Vis spectrophotometer equipment Shimadzu model UV-1800 (Barueri, Brazil), it was possible to find 498 nm as maximum absorption of the CR, a value confirmed in the literature.[18]

Studies of the effect of medium pH and adsorbent mass on CR removal using the three calcined materials were also carried out. The study of the pH of the medium used 20 mL of the CR aqueous solution at a concentration of 30 ppm and 20 mg of the adsorbent material. Adjustments of the pH (1, 3, 5, 7, 9 and 11) of the CR solution were performed using aqueous solutions of 0.1 mol L^{-1} NaOH (Synth, São Paulo, Brazil) and 0.05 mol L^{-1} HCl (Neon, São Paulo, Brazil). The mass study was carried out with 20 mL of the CR solution (30 ppm) and with the masses of 10, 20 and 30 mg of the adsorbent materials. Both studies were made kept the system under magnetic stirring for 1 h and 30 min and the resulting solutions were filtered and analyzed under the same conditions used to obtain the analytical curve. The medium pH and adsorbent mass studies were performed in triplicate to minimize errors. Then, the adsorption tests were carried out in a shaking water bath from Tecnal's stirring and heating control at a temperature of 30, 40 and 50 °C, using 125 mL Erlenmeyer flasks containing 10 mg of the adsorbent mass previously dried in an oven for 30 min at 60 °C and 20 mL of Congo Red solution at a concentration of 30 ppm. The contact times were 10, 20, 30, 50, 70, 90 and 120 min. After these times, the systems were subjected to common filtration and the resulting solution was subjected to analysis by absorption spectrophotometry in the UV-Vis region under the same conditions used in the reference solution. The adsorption experiments were performed in triplicate without correction of the pH of the medium. The pH of the system was measured at the beginning and end of each procedure, keeping it constant at pH = 5. The experimental conditions were proposed with base in preliminary studies and other works.[4-6] The values of removal efficiency (E, in %) and the amount of CR adsorbed (q) in milligrams *per* gram of adsorbent were calculated.[4,6] The kinetic model of variable constants (VC) was used for the kinetic study of the adsorption, using the equations presented by Lemos *et al.*[4]

Recovery and reuse of the adsorbents used

The materials recovered in the adsorption tests by contact time (about 150 mg of the material loaded with CR compound) were dried in an oven at 60 °C for 30 min (method 1). Of this material, 50 mg was submitted to the calcination process at 900 °C for 2 h (method 2). The other 100 mg of each material were submitted directly to the cycle reuse study.

The study of reuse in cycles was carried out in a shaking water bath from Tecnal's and heating control at 30 °C in Erlenmeyer flasks containing 20 mL of dye solution at 30 ppm and 100 mg of adsorbent material (obtained by method 1 of recovery). The system

was subjected to stirring for 1 h and 30 min. At the end of time, the system was subjected to the filtration process and the solution obtained was analyzed by UV-Vis absorption spectroscopy under the same conditions described above. The resulting filtrate was again dried in an oven at 60 °C for 30 min and, soon after, the mass obtained, 80 mg, was applied in a new reuse cycle with the same conditions described above. The same procedure was repeated using 50 mg and then 20 mg of the adsorbent material.

At the same time, the same study was carried out using 50 mg of the recovered and regenerated material (obtained by method 2 that was submitted to the calcination process), in a shaking water bath from Tecnal's and heating control at 30 °C in Erlenmeyer flasks containing 20 mL of dye solution at 30 ppm and test time of 1 h and 30 min.

The materials recovered and dried in an oven at 60 °C for 30 min (method 1) were named LZOR1, LNZOR1 and LFZOR1 and those that, in addition to drying, were also subjected to calcination at 900 °C for 2 h (method 2) were named LZOR2, LNZOR2 and LFZOR2. The materials recovered in methods 1 and 2 were characterized by X-ray diffraction (XRD) powder method.

Study using an industrial effluent

The adsorbent materials obtained from the synthesis process were submitted to the study of removal of textile dyes from industrial effluent. For this procedure, 1 L of red industrial effluent obtained after the dyeing process in a small fabric industry located in Sergipe, Brazil, was collected. The pH measured at the time of collection was pH = 7. The sample was sent to the laboratory for studies.

For the study, the sample was diluted with distilled water in a 1:1 ratio, then it was analyzed in a UV-Vis spectrophotometer Shimadzu model UV-1800, and the scan was applied in the range of 400 to 700 nm. A study of the stability of the dye from industrial effluent under visible light and stirring of the solution was carried out at times of 0, 5, 15, 30, 60, 90, 120 and 150 min, without the presence of adsorbent. For the textile dye adsorption study, 10 mg of the adsorbent material previously dried in an oven at 60 °C for 30 min and 20 mL of the textile dye solution were used. The system (adsorbent/adsorbate) was kept under magnetic stirring for 120 min. Then, the solution was filtered and analyzed in a UV-Vis spectrophotometer under the same conditions used and described above.

The study was carried out with calcined materials (LZO900, LFZO900 and LNZO900), with precursor powders (LZO350, LFZO350 and LNZO350), with commercial activated carbon (Synth, São Paulo, Brazil) and with commercial silica gel (Carvalhaes, Porto Alegre, Brazil). To minimize errors, the study was performed in triplicate.

RESULTS AND DISCUSSION

Synthesis of the $La_2Zr_2O_7$ and $La_2M_{0.3}Zr_{1.7}O_7$ (M = Fe or Ni)

Through XRD analysis, it was possible to observe that there was no crystalline phase formation in the LZO350 material (Figure 1a), indicating the amorphous condition of this material, an expected behavior since in the literature there were no reports of obtaining a crystalline structure for this type of mixed oxides at this temperature.

The XRD patterns of the calcined materials at 900 °C (Figure 1b) confirm the obtainment of the $La_2Zr_2O_7$ phase with a pyrochlore structure of cubic symmetry in the three materials, LZO900, LNZO900 and LFZO900, whose main peaks are shown at 2θ = 28.60°; 33.20°; 47.60° and 56.50° and are in accordance with standard ICSD letter No. 180491 and Hagiwara *et al.*[16]

In the materials doped with iron (LFZO) or nickel (LNZO) it is possible to notice that in addition to the $La_2Zr_2O_7$ (pyrochlore phase), the presence of secondary phases is also observed. It is also possible to note that there were no significant displacements or the disappearance of the peaks referring to the $La_2Zr_2O_7$ phase.

XRD pattern of LFZO showed peaks of secondary phases of low intensity at 2θ = 31.84° referring to zirconium oxide (ZrO_2) (ICSD 647689) and at 2θ = 45.84° referring to lanthanum oxide (La_2O_3) (ICSD 7795). In the LNZO material, secondary phase peaks at 2θ = 43.16° related to nickel oxide (NiO) (ICSD 9866) was identified.

The presence of secondary phases may be indicative of excess/deficiency of reagents and/or due to incompatibility of doping ions for the structure, or even the possibility of forming a more stable structure. The results suggest that possibly the stoichiometry of the reagents is not completely suitable for reactions in the solid state.

Some works[2,19,22] reported the use of other methods for the synthesis of the $La_2Zr_2O_7$ material (with and without doping), which, however, did not prove to be as effective in obtaining the phase in relation to the proteic method related in this work. The modified proteic method has been proving to be effective in the formation of the mixed oxides phase, in addition to presenting other advantages such as low cost, lower processing temperatures, and obtaining well crystallized materials.

The average size of the crystallites of pyrochlore phase in the materials were calculated, in addition, the surface area and the PZC values were also determined. Table 1 shows the values obtained.

It is possible to observe that the three prepared materials presented very close average crystallite size values (of $La_2Zr_2O_7$ phase), being 15 nm for LFZO and LNZO and 18 nm for LZO. These values of SSA and mean crystallite size are excellent results if compared with that data obtained from the literature[22] that obtained the $La_2Zr_2O_7$

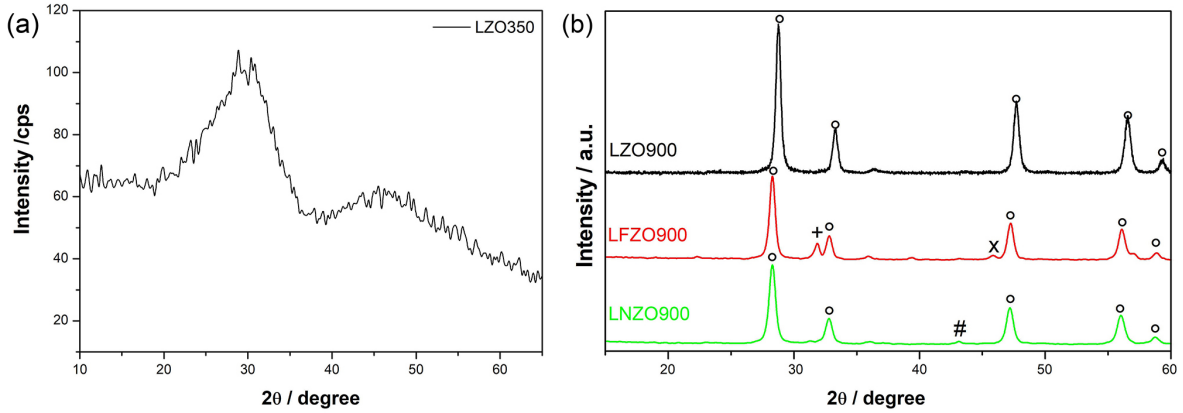

Figure 1. *XRD patterns for (a) LZO350 and (b) LZO900, LFZO900 and LNZO900 materials. ○: $La_2Zr_2O_7$; +: ZrO_2; ×: La_2O_3; #: NiO*

Table 1. Properties of the adsorbents obtained, LZO, LFO and LNZO

	LZO	LFZO	LNZO
Crystallite size / nm	18	15	15
SSA / ($m^2 g^{-1}$)	23	29	22
PZC	6.3	5.5	6.1

SSA: specific surface area; PZC: point of zero charge.

material by the modified Pechini method with a mean crystallite size of 46.9 nm and surface area of 1.35 $m^2 g^{-1}$. This observation is important since the size of the crystallites is directly related to some properties of the materials, where materials with smaller crystallite sizes generally have a greater surface area, which facilitates the interaction of the adsorbent surface with the adsorbate.[23]

In the synthesis of the materials, collagen was used, which is a protein made up of amino acids and presents an amino and carboxyl group that are linked to the same carbon atom. In the FTIR spectra of the heat-treated and calcined material, the bands are compared with those of collagen (Figure 1S, Supplementary Material). The FTIR spectra for the LZO material heat treated at 350 °C and calcined at 900 °C (Figure 1S) indicate that after the heat treatment and calcination process it is still possible to notice a broad band in the region between 3500-3000 cm^{-1} referring to the stretching vibration of the O–H bond, and a band referring to N–H in the region between 1640 and 1550 cm^{-1}. Furthermore, characteristic bands originating from collagen observed in the range of 1100 to 1640 cm^{-1} are attenuated in the materials after heat treatment and calcination, which may be an indication of the interaction between the ionic species present in the solution with species of the collagen structure, as shown in previously reported.[4-6] In the spectrum of the material calcined at 900 °C, the stretching band of the M–O bond (close to 550 cm^{-1}) was more evident when compared with the spectrum of the material heat-treated at 350 °C, which suggests that calcination at 900 °C leads to the formation of oxides.

The results also showed in Table 1 indicate that the PZC values of the materials were close to 6. If the pH value of the PZC is greater than the pH value of the medium, the surface of the material becomes positively charged, which favors the adsorption of negatively charged particles, anionic species. Otherwise, there will be a tendency to adsorb positively charged species, cationic species.[4,11,24] One of the mechanisms involved in the adsorption process is the electrostatic interaction that can occur between positively charged sites of the adsorbent material and negatively charged species present in the dye. When the pH increases, the number of these positively charged sites decreases, increasing the negatively charged sites and, consequently, reducing dye adsorption due to electrostatic repulsion.[25] As the Congo Red dye is considered an anionic species, its adsorption will occur favorably when the pH of the medium is lower than the pH of the PZC. This fact was confirmed in preliminary tests, which revealed that the ability to remove Congo Red dye increased as the pH of the solution decreased.

The SEM images (Figure 2) show that the prepared adsorbents present the formation of aggregated particles with irregular morphology and size variation. It is also possible to notice the presence of pores of different sizes in its structure. This may show a characteristic that favors the adsorption process.

This same behavior was observed in the literature,[22,26] that obtained materials with a pyrochlore structure which also formed aggregated particles with irregular morphology and varied pore sizes.

Contaminant removal tests from the aqueous media

To carry out the adsorption tests using Congo Red as model compound[7,21] (Figure 3), the effects of the pH of the medium and the mass of the adsorbent with the materials obtained were initially investigated. Figure 3a shows the values of removal efficiency (%) of the CR compound at different pH of the medium.

It was possible to verify that as the pH of the medium increases, there is a decrease in the CR removal efficiency. This behavior does not deviate from expectations since the zero-charge point is around 6, and as the Congo Red is an anionic species, its adsorption occurs favorably when the pH of the medium is lower than the PCZ.

For pH 1 and 3, the efficiency of CR removal from the medium in the three materials was practically the same, with efficiency above 98%. For pH 5 and 7, it is possible to notice a drop in the efficiency values, mainly when LZO material was used, which presented efficiency around 60% at pH = 5. As the pH of the medium becomes more basic, the removal efficiency becomes lower, however, the LZO material shows some stability at pH above 7, while when is used the LFZO and LNZO materials showed the greatest drops in removal efficiency.

It is reported in the literature[7,18,27] that the Congo Red compound presents better adsorption when the pH of the medium in which it is worked is in pH ranges below 6. This is mainly due to the surface charge of the solid, which varies with the pH of the medium. At more acidic pH, the surface of the solid is positively charged, which favors the adsorption process of anionic species, such as the CR compound.

The values of removal efficiency (%) of the CR when used different mass of adsorbents (Figure 3b) indicate that the increase in the mass of the adsorbent directly represents an increase in the efficiency of CR removal. However, it is important to highlight that the increase in efficiency was not as significant when comparing the use of the LFZO and LNZO materials in the 20 and 30 mg masses. The LFZO material, which showed low efficiency at a mass of 10 mg when compared directly with LNZO, showed better efficiency in increasing the adsorbent mass.

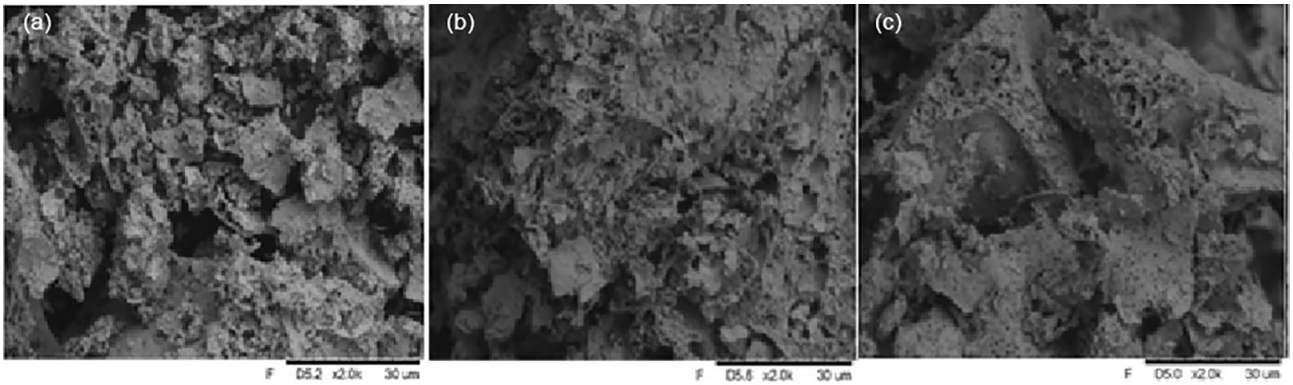

Figure 2. *SEM images of prepared adsorbents: (a) LZO; (b) LFZO and (c) LNZO*

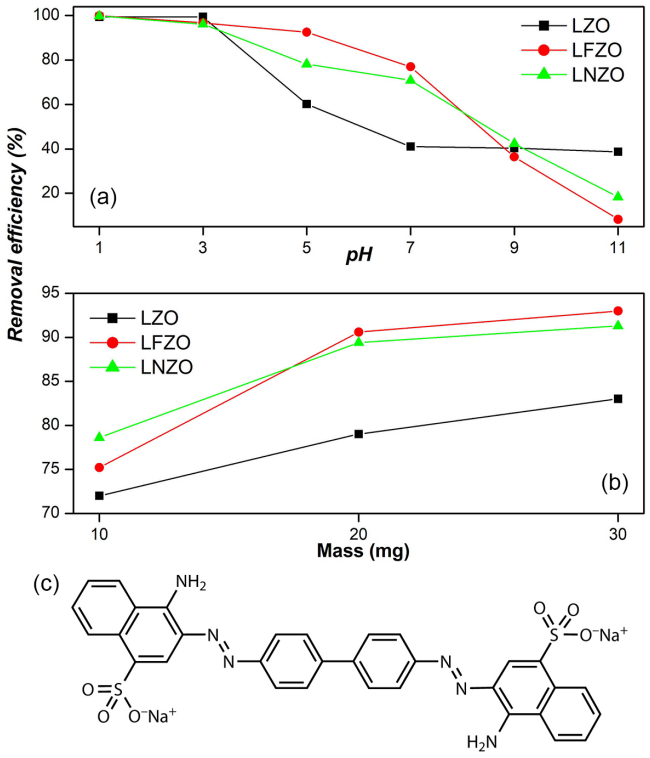

Figure 3. *Removal efficiency of CR at (a) different pH of the medium and at (b) different adsorbent mass used; (c) structure of Congo Red compound*

The results of the study of the efficiency of CR removal as a function of contact time (Figure 4a) indicate that the three adsorbent materials have high efficiency of compound removal.

It is possible to observe that the efficiency of CR removal when temperature of system is at 30 °C occurs quickly in the first minutes of contact and remains constant, showing a subtle improvement in the adsorption at 90 and 120 min, which is an indication that there was an equilibrium in this process. By increasing the temperature to 40 °C it is possible to notice a reduction in the removal efficiency (Figure 4b). This reduction is more pronounced when LZO material was used, followed by the LNZO material. The LFZO material showed a reduction in the adsorptive capacity, but still showing a better result compared to the others.

By increasing the system temperature to 50 °C, it is possible to notice that the CR removal efficiency is similar to that presented at a temperature of 40 °C and for all adsorbents. The reduction in CR removal efficiency with increasing temperature is a trend discussed in the literature. With increasing temperature, a decrease in adsorption may occur, mainly due to the weakening of the adsorption forces. The reduction in adsorption with increasing temperature can be caused due to weaker adsorption forces between the active sites of the adsorbent and the adsorbate species.[28] These effects suggest that the adsorption mechanism may involve an electrostatic interaction that is generally associated with low heat of adsorption,[29] that is, the adsorption process has an exothermic characteristic.[30]

Evaluating the results obtained from the amount of adsorbed CR compound and comparing it at the same temperature, it can be seen that the LFZO adsorbent presented the best result when the test was conducted at a temperature of 40 °C, while the LNZO material presented the best result at the temperature of 50 °C test. Similar behavior was observed to the adsorption efficiency (E, in %) in the maximum time of 120 min and at a temperature of 50 °C where LNZO showed better results followed by LFZO and LZO. At the test temperature of 30 °C, the three adsorbents showed the same

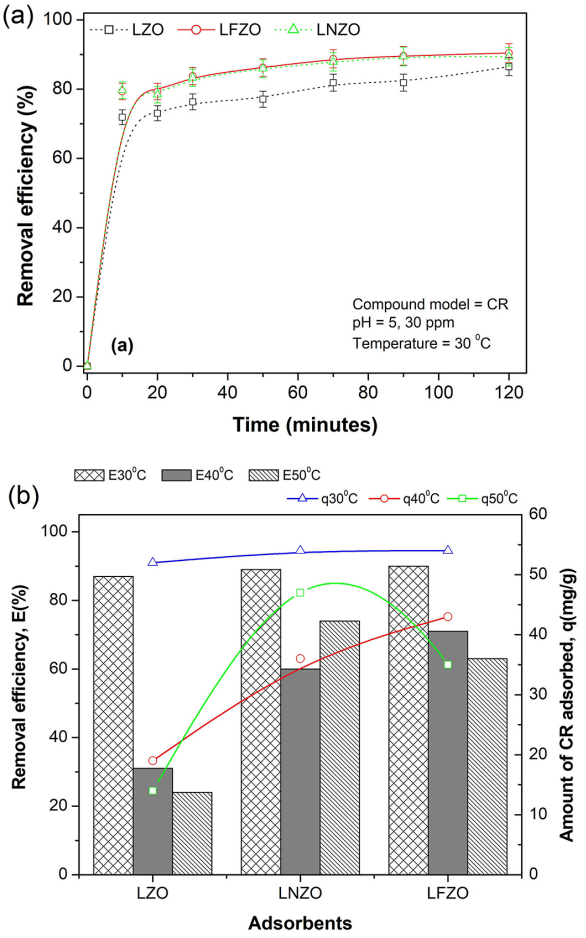

Figure 4. *(a) Congo Red removal efficiency (E, in %) using LZO, LNZO and LFZO materials as a function of contact time; (b) amount of CR adsorbed (q, mg g^{-1}) and E(%) at equilibrium time at different temperatures (30, 40 and 50 °C)*

adsorption efficiency, since adsorption follows a trend in which its efficiency becomes greater as there is an increase in mass transfer from the CR solution to the adsorbent material, consequently decreasing its concentration.[31]

The kinetic study was applied using pseudo first order (PFO), pseudo second order (PSO) and variable constant (VC) models. All applied kinetic models presented a good fit, but overall, the VC model describes the results more closely (Table 1S, Supplementary Material). The parameters obtained by VC model for the adsorption kinetics of the CR by the LZO, LFZO and LNZO materials are presented in Table 2. Due to the good fit to this model, it can be inferred that fractional reactions occur, which suggests that the concentration of the reagents changes significantly during the reaction and that the adsorption velocity constant (K_{AV}) values are high, indicating that the reaction speeds are faster.[32]

The results show that the insertion of iron or nickel ions in the composition of the mixed oxide results in a more efficient material to removal CR compound at any temperature of the system that was studied. This suggests that doping of different ions in the composition of the structure not only results in a more efficient material, but also a more stable one.

Recovery and reuse of the adsorbents used

Figure 5a presents the results obtained in the study of reuse in cycles using the materials obtained after the adsorption tests, dried

Table 2. Parameters obtained by kinetic model of variable constants (VC) for the adsorption of Congo Red (CR) on materials at temperatures of 30, 40 and 50 °C

Parameter	T = 30 °C			T = 40 °C			T = 50 °C		
	LZO	LFZO	LNZO	LZO	LFZO	LNZO	LZO	LFZO	LNZO
q / (mg g^{-1})	50.61	54.03	52.23	17.71	44.41	41.99	15.46	37.46	45.66
k_{AV}	0.967	0.560	1.036	0.243	0.443	0.226	1.237	1.001	0.391
R^2	0.989	0.997	0.990	0.992	0.998	0.997	0.991	0.998	0.996
χ^2	4.014	1.502	4.590	0.433	0.520	0.681	0.299	0.452	1.198
n	0.271	0.364	0.303	0.591	0.293	0.201	0.502	0.370	0.299

q: maximum adsorption capacities; k_{AV}: adsorption velocity constant; R^2: correlation coefficient; χ^2: chi-square; n: adjustment parameter.

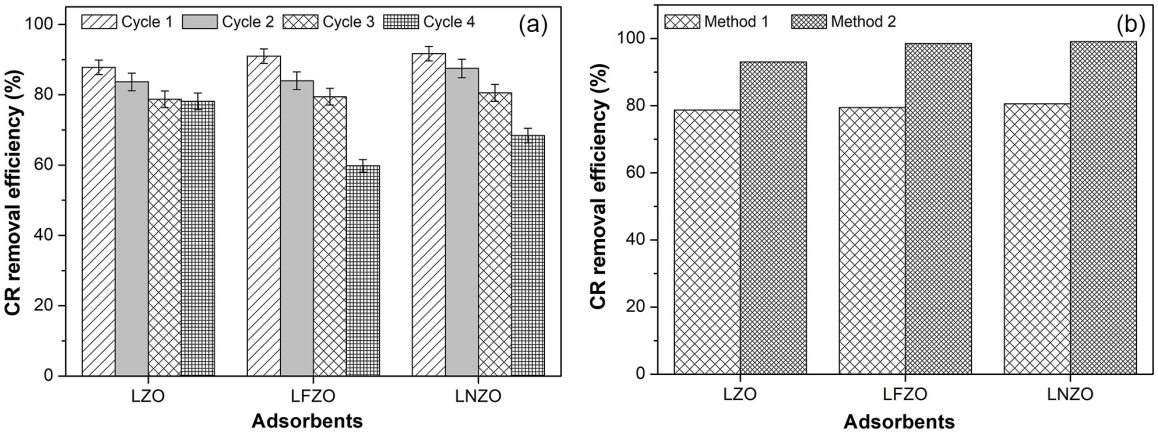

Figure 5. *CR removal efficiency (%) using materials submitted to reuse in cycles (a) and comparison of CR removal efficiency (%) under materials using different recovery and reuse methodologies (b)*

at 60 °C for 30 min and that were again submitted to the adsorption process.

The adsorptive capacity of the materials applied in the cycle of reuse decreased as the mass of adsorbent used in each cycle decreased. It is possible to verify that the LZO material showed linearity in its adsorptive capacity even with the decrease in mass, a behavior that was not observed for the LFZO and LNZO materials, which had a more significant reduction in their adsorptive capacities as the adsorbent mass decreased. An expected behavior was the decrease in adsorption efficiency with decreasing mass, since in the system there are fewer active sites available for the adsorption process to occur.[12]

Figure 5b presents the results obtained in the study comparing the methodology for recovering and reusing adsorbents. In method 1, the adsorbent recovered from the adsorption tests was only dried in an oven at 60 °C for 30 min. In method 2, in addition to drying, the adsorbent was subjected to calcination at 900 °C for 2 h.

In this case, there is an indication that the materials presented stability after the adsorption tests and that they can be submitted to a new adsorption process. It is possible to notice that the calcination process (method 2) increased the adsorption efficiency of the materials. However, this efficiency is not far from that presented by materials that have not gone through the calcination process. This demonstrates that the raw materials obtained after an adsorption process can be applied again in reuse cycles, maintaining their high adsorption efficiency.

The results demonstrate that the adsorption of the Congo Red compound in the first use and in the use in cycles using the pyrochlore structure materials, synthesized by the modified proteic method, was efficient and that they can be influenced mainly in the type of structure that has vacancies in which they allow that adsorption processes may occur.

After carrying out the adsorption tests, it was verified whether the pyrochlore structure was maintained and the possibility of recovery and reuse. The systems obtained (adsorbate/adsorbent) after the adsorption tests were subjected again to characterization techniques by XRD. Data analysis allowed verifying if the pyrochlore structure was maintained in the materials after the adsorption studies. This is of great importance, since maintaining the structure and reusing materials in new adsorption tests avoids additional costs and helps to reduce waste generation.

Figure 6 presents the X-ray diffractograms of the materials recovered after the adsorption tests, which were named LZO-R, LFZO-R and LNZO-R, where R refers to recovered.

From X-ray diffractograms (XRD) in Figure 6, it is possible to verify that the pyrochlore structure ($La_2Zr_2O_7$) was maintained in the three materials, in addition to the presence of two secondary phases in the material doped with iron (LFZO), at $2\theta = 31.84°$ referring to zirconium oxide (ZrO_2) and $2\theta = 39.30°$ referring to lanthanum oxide (La_2O_3), phases that were also identified in the material before the adsorption tests.

Other secondary phases of low intensity that were identified in the materials before the adsorption tests were not identified in the materials after the tests. It was also possible to observe that there was no displacement or disappearance of the peaks referring to the $La_2Zr_2O_7$ phase in the materials. The results indicate that the structure of the materials is preserved and maintained after the adsorption tests.

Study using an industrial effluent

With the objective of evaluating the efficiency of materials with a pyrochlore structure obtained by the modified protein method in the adsorption of textile dye from industrial effluent, an adsorption study was carried out using the synthesized materials, in addition to a comparison with other commercially used adsorbent.

One of the main characteristics of the currently used textile dyes is their color stability, since the dyes must be able to fix themselves

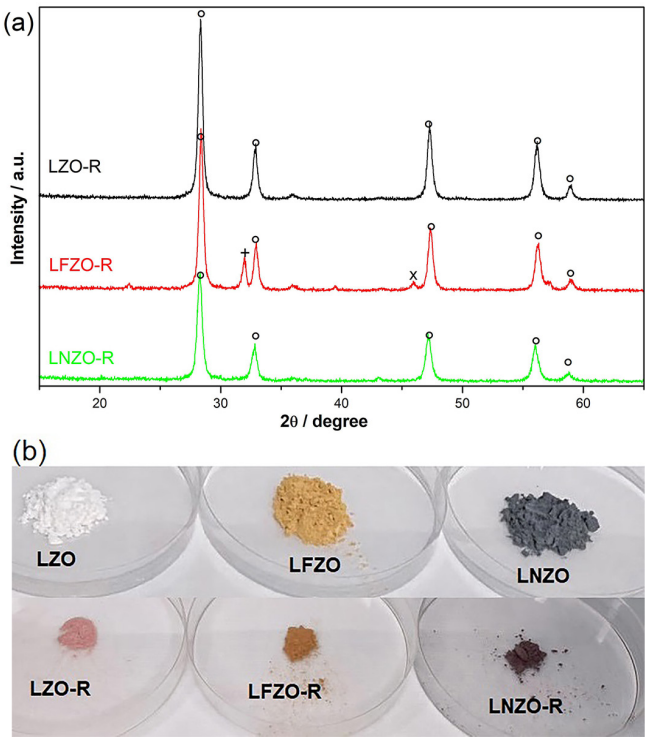

Figure 6. *(a) XRD patterns of the recovered materials after adsorption tests, ○: $La_2Zr_2O_7$; +: ZrO_2; ×: La_2O_3; (b) image of the materials as synthesized and recovered*

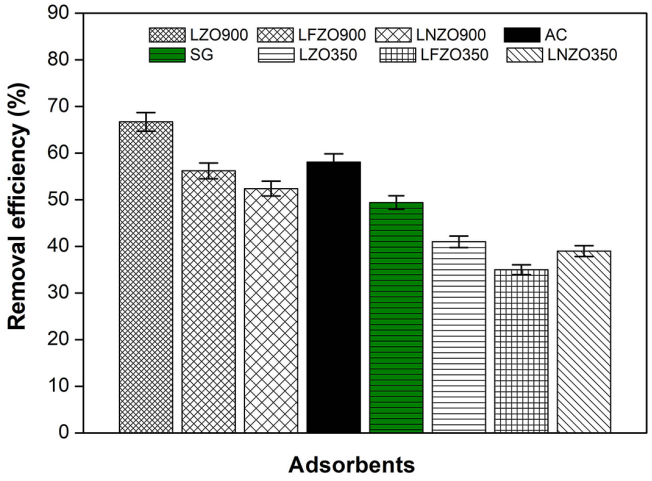

Figure 7. *Efficiency of dye removal from industrial effluent using different materials*

permanently in the fibers of the fabrics. Thus, a study was conducted to evaluate the photo stability of the collected industrial effluent in order to investigate whether it suffers any degradation of its structure and color when exposed to visible light and agitation. The UV-Vis spectra obtained (Figure 2S, Supplementary Material) indicated that the red dye collected from an industrial effluent did not change under the influence of visible light and agitation because the maximum band observed at 498 nm did not change, therefore the compounds does not undergo photodegradation under these conditions. This result was already expected, as it is known that dyes in aqueous media are stable, but it reinforces the idea that the presence of these contaminants in effluents represents a high risk to the environment, as previously described.[33]

Considering that the industrial dye collected from an effluent does not show degradation under the influence of visible light during the study time, in this study different materials were evaluated in the removal of the dye by adsorption. Figure 7 presents a comparison of the results of the study of dye removal from industrial effluent using different adsorbent materials: LZO900, LFZO900, LNZO900, commercial activated carbon (AC) and commercial silica gel (SG). This study was also carried out with the precursor powders of the materials LZO900, LFZO900 and LNZO900, respectively LZO350, LFZO350 and LNZO350.

It is observed that the LZO900 material presented the best result in removing the industrial dye in comparison to other adsorbents synthesized (LFZO900, LNZO900). As expected, activated carbon and silica gel also showed high efficiency to remove the red dye. It is noteworthy that all materials were efficient in the red dye adsorption process with relatively close efficiencies.

The precursor powders of the materials did not show the efficiency of removing the dye from the industrial effluent as high as the calcined materials. The results suggest that there may be an influence of the crystalline structure formed on the dye removal efficiency. LZO350, LFZO350 and LNZO350 materials were treated at a temperature of 350 °C and, in this condition, a crystalline structure of mixed oxides was not formed, and the adsorbate/adsorbent interaction was not as effective as in calcined adsorbents.

A relevant observation to be made is that the LZO900 material showed adsorption efficiency equivalent to an industrially used material, which is activated carbon and silica gel, commonly used in industrial effluent treatment plants.[34] Some these adsorbents used commercially, despite its significant advantages, presents some limitations, such as high cost, difficulty in regeneration and final disposal.[7,35,36] This fact was not observed in materials with a pyrochlore structure obtained by the low-cost method of this work, the modified proteic method, which proved to be efficient materials in the removal of textile dyes, in addition to presenting the possibility of reuse in cycles, maintaining high efficiency without the need for additional steps.

CONCLUSIONS

The syntheses of the $La_2Zr_2O_7$ and $La_2M_{0.3}Zr_{1.7}O_7$ (M = Fe or Ni) were successful, generating their respective nanomaterials with a pyrochlore structure with a cubic structure. Compared to other works reported in the literature, the modified proteic method proved to be very promising in phase formation by employing a low-cost chelating agent, fewer reaction steps, lower processing temperatures and obtaining well-crystallized materials with an average size of crystallite around 16 nm, values much lower than reported for this type of material. The micrographs showed materials with irregular morphology and pores in their structure, and the materials had a total area of around 25 $m^2\ g^{-1}$, which are significantly larger values than reported for this type of material. The obtained materials proved to be effective in Congo Red removal studies from the water without the need for pH adjustments in the medium, with efficiency values ranging between 79 and 93%. The CR removal efficiency decreased with increasing test temperature when using LZO and LFZO materials. The LNZO material showed the best CR removal results at a temperature of 50 °C. The materials showed excellent results in the cycle reuse study, highlighting the LZO material (E > 80%) that maintained the CR removal efficiency even with the mass decrease for four cycles. In comparison with the material that went through the calcination process again, the results were equivalent, which indicates that there is stability in the materials obtained and that they do not need a new calcination process to maintain their adsorptive activities. The pyrochlore structure of the LZO, LNZO and LFZO materials is maintained after the adsorption tests. All materials with a

pyrochlore structure obtained in this work also proved to be efficient materials in the removal of textile dyes from industrial effluents and with efficiency values close than the adsorbent typically used as commercial active carbon.

SUPPLEMENTARY MATERIAL

Complementary material for this work is available at http://quimicanova.sbq.org.br/, as a PDF file, with free access.

ACKNOWLEDGMENTS

The authors would like to thank CNPq for the fundamental financial support for the development of this research. This work was carried out with the support of the CAPES (Financing Code 001) and to CLQM (Multi-user Chemical Laboratory Center) of the Federal University of Sergipe for the support and analytical infrastructure provided.

REFERENCES

1. Moure, C.; Peña, O.; *Prog. Solid State Chem.* **2015**, *43*, 123. [Crossref]
2. Resende, K. A.; Ávila-Neto, C. N.; Rabelo-Neto, R. C.; Noronha, F. B.; Hori, C. E.; *Catal. Today* **2015**, *242*, 71. [Crossref]
3. Rangel, M. C.; Querino, O. S.; Borges, S. M. S.; Marchetti, S. G. M.; Assaf, J. M.; Vásquez, D. P. R.; Rodella, C. B.; Silva, F.; Silva, A. H. M.; Ramon, A. D.; *Catal. Today* **2017**, *296*, 262. [Crossref]
4. Lemos, J. A. S.; Ribeiro, I. A.; Souza, M. J. B.; Pedrosa, A. M. G.; *J. Braz. Chem. Soc.* **2023**, *34*, 36. [Crossref]
5. Nascimento, É. V.; Pedrosa, A. M. G.; Souza, M. J. B.; *Water Sci. Technol.* **2021**, *83*, 2793. [Crossref]
6. Santos, A. G.; Leite, J. O.; Souza, M. J. B.; Gimenez, I. F.; Pedrosa, A. M. G.; *Ceram. Int.* **2018**, *44*, 5743. [Crossref]
7. Wang, L.; Li, J.; Wang, Y.; Zhao, L.; *J. Hazard. Mater.* **2011**, *196*, 342. [Crossref]
8. Gade, R.; Ahemed, A.; Yanapu, K. L.; Abate, S. Y.; Tao, Y.-T.; Pola, S. J.; *J. Environ. Chem. Eng.* **2018**, *6*, 4504. [Crossref]
9. Vörösmarty, C. J.; McIntyre, P. B.; Gessner, M. O.; Dudgeon, D.; Prusevich, A.; Green, P.; Glidden, S.; Bunn, S. E.; Sullivan, C. A.; Liermann, C. R.; Davies, P. M.; *Nature* **2010**, *467*, 555. [Crossref]
10. Zanoni, M. V. B.; Yamanaka, H.; *Corantes: Caracterização Química, Toxicológica, Métodos de Detecção e Tratamento*, 1st ed.; Cultura Acadêmica: São Paulo, 2016.
11. Ribeiro, I. A.; Lemos, J. A. S.; Souza, M. J. B.; Pedrosa, A. M. G.; *Int. J. Mater. Res.* **2022**, *113*, 871. [Crossref]
12. Tavakkoli, H.; Hamedi, F.; *Res. Chem. Intermed.* **2016**, *42*, 3005. [Crossref]
13. Ribeiro, J. F. S.; Souza, A. A.; Lima, E. C. N. L.; Souza, M. J. B.; Souza, A. M. G. P.; *Sci. Plena* **2021**, *16*, 127202. [Crossref]
14. Eyring, L.; O'Keeffe M.; *The Chemistry of Extended Defects in Non-Metallic Solids*, 1st ed.; Institute for Advanced Study on the Chemistry of Extended Defects in Non-Metallic Solids: Amsterdam, 1970.
15. Nishino, H.; Yamamura, H.; Arai, T.; Kakinuma, K.; Nomura, K.; *J. Ceram. Soc. Jpn.* **2004**, *112*, 541. [Crossref]
16. Hagiwara, T.; Yamamura, H.; Nomura, K.; Igawa, M.; *J. Ceram. Soc. Jpn.* **2013**, *121*, 205. [Crossref]
17. Santos, J. C.; Souza, M. J. B.; Mesquita, M. E.; Pedrosa, A. M. G.; *Sci. Plena* **2012**, *8*, 037202. [Link] accessed in July 2024
18. Souza, A. A.; Fernandes, J. B. R.; Ribeiro, J. F. S.; Souza, M. J. B.; Pedrosa, A. M. G.; *Cerâmica* **2021**, *67*, 406. [Crossref]
19. Rao, K. K.; Banu, T.; Vithal, M.; Swamy, G. Y. S. K.; Kumar, K. R.; *Mater. Lett.* **2002**, *54*, 205. [Crossref]
20. Haynes, D. J.; Berry, D. A.; Shekhawat, D.; Spivey, J. J.; *Catal. Today* **2008**, *136*, 206. [Crossref]
21. Saikia, P.; Miah, A. T.; Das, P. P.; *J. Chem. Sci.* **2017**, *129*, 81. [Crossref]
22. Gaur, S.; Haynes, D. J.; Spivey, J. J.; *Appl. Catal., A* **2011**, *403*, 142. [Crossref]
23. Melo, D. Q.; Lima, A. C. A.; Vidal, C. B.; Raulino, G. S. C.; Nascimento, R. F. In *Adsorção: Aspectos Teóricos e Aplicações Ambientais*; Guimarães, A. C. L., ed.; Imprensa Universitária: Fortaleza, 2014.
24. de Paula, L. N. R.; de Paula, G. M.; Rodrigues, M. G. F.; *Cerâmica* **2020**, *66*, 269. [Crossref]
25. Debrassi, A.; Largura, M. C. T.; Rodrigues, C. A.; *Quim. Nova* **2011**, *34*, 764. [Crossref]
26. Park, S.; Hwang, H. J.; Moon, J.; *Catal. Lett.* **2003**, *87*, 219. [Crossref]
27. Chatterjee, S.; Lee, D. S.; Lee, M. W.; Woo, S. H.; *Bioresour. Technol.* **2009**, *100*, 3862. [Crossref]
28. Abdelwahab, O.; Fouad, Y. O.; Amin, N. K.; Mandor, H.; *Environ. Prog. Sustainable Energy* **2015**, *34*, 351. [Crossref]
29. Karaca, S.; Gürses, A.; Ejder, M.; Açıkyıldız, M.; *J. Hazard. Mater.* **2006**, *128*, 273. [Crossref]
30. Kula, I.; Uğurlu, M.; Karaoğlu, H.; Çelic, A.; *Bioresour. Technol.* **2008**, *99*, 492. [Crossref]
31. Zhao, M.; Yuan, Q.; Zhang, H.; Li, C.; Wang, Y.; Wang, W.; *J. Alloys Compd.* **2019**, *782*, 1049. [Crossref]
32. Cardoso, N. F.; Pinto, R. B.; Lima, E. C.; Calvete, T.; Amavisca, C. V.; Royer, B.; Cunha, M. L.; Fernandes, T. H. M.; Pinto, I. S.; *Desalination* **2011**, *269*, 92. [Crossref]
33. Liu, J.; Wang, N.; Zhang, H.; Baeyens, J.; *J. Environ. Manage.* **2019**, *238*, 473. [Crossref]
34. de Farias, R. S.; Buarque, H. L. B.; da Cruz, M. R.; Cardoso, L. M. F.; Gondim, T. A.; de Paulo, V. R.; *Eng. Sanit. Ambiental* **2018**, *23*, 1053. [Crossref]
35. Tor, A.; Cengeloglu, Y.; *J. Hazard. Mater.* **2006**, *138*, 409. [Crossref]
36. Zhu, H.-Y.; Fu, Y.-Q.; Jiang, R.; Jiang, J.-H.; Xiao, L.; Zeng, G.-M.; Zhao, S.-L.; Wang, Y.; *Chem. Eng. J.* **2011**, *173*, 494. [Crossref]